
Subject-specific quantitative susceptibility mapping using patch based deep image priors

Arvind Balachandrasekaran, Davood Karimi, Camilo Jaimes, Ali Gholipour

Computational Radiology lab

Harvard Medical School

Boston, MA 02115

arvind.balachandrasekaran, davood.karimi@childrens.harvard.edu

camilo.jaimescobos, ali.gholipour@childrens.harvard.edu

Abstract

Quantitative Susceptibility Mapping is a parametric imaging technique to estimate the magnetic susceptibilities of biological tissues from MRI phase measurements. This problem of estimating the susceptibility map is ill posed. Regularized recovery approaches exploiting signal properties such as smoothness and sparsity improve reconstructions, but suffer from over-smoothing artifacts. Deep learning approaches have shown great potential and generate maps with reduced artifacts. However, for reasonable reconstructions and network generalization, they require numerous training datasets resulting in increased data acquisition time. To overcome this issue, we proposed a subject-specific, patch-based, unsupervised learning algorithm to estimate the susceptibility map. We make the problem well-posed by exploiting the redundancies across the patches of the map using a deep convolutional neural network. We formulated the recovery of the susceptibility map as a regularized optimization problem and adopted an alternating minimization strategy to solve it. We tested the algorithm on a 3D in vivo dataset and, qualitatively and quantitatively, demonstrated improved reconstructions over competing methods.

1 Introduction

Quantitative Susceptibility Mapping (QSM) is a parametric imaging technique to estimate the magnetic susceptibilities of biological tissues. It enables quantification of iron concentration in gray matter [1], myelin content in white matter [2], deoxyhemoglobin in veins [3] etc. Changes in the concentrations reflect an underlying pathology, which include micro bleeds [4], hemorrhages [5] and neurodegenerative diseases [6, 7], and can potentially be used as a bio-marker [8].

The susceptibility map is related to phase measurements through a 3D convolution with a dipole kernel. However, the problem of estimating the map through direct inversion is ill posed and results in streaking artifacts. To improve the quality of reconstructions, regularized recovery approaches enforcing signal sparsity and smoothness have been introduced [9, 10]. These approaches reduce the streaking artifacts but introduce blurring in the recovered maps. Recently, supervised deep learning methods have shown great potential and have generated maps with reduced artifacts [11]. However, to achieve reasonable reconstruction quality and for the network to generalize well to unseen data, these approaches require a lot of training data, which result in increased data acquisition time.

We propose a subject-specific, patch-based, unsupervised deep learning algorithm to estimate the susceptibility map from phase measurements. Patch based priors have been successful in many image restoration tasks including recovery of MR images from undersampled measurements [12]. To make the problem well-posed, we exploit the redundancies across the different patches in the map using a deep convolutional neural network (CNN). The recovery of the map is then posed as a regularized

optimization problem, where the representation of different patches by the deep neural network acts as a regularizer. We propose an alternating minimization strategy to solve the optimization problem and recover the susceptibility map. While the algorithm is developed for the QSM application, the proposed framework can be applied to solve any general linear inverse problem characterized by a forward model, of which denoising happens to be a special case [13]. We tested the algorithm on an in vivo 3D Gradient echo dataset that was provided as part of a QSM reconstruction challenge [14]. We demonstrated improved QSM reconstructions, both quantitatively and qualitatively, over competing methods.

2 Methods

The forward model relating the magnetic resonance (MR) tissue phase $\Phi \in \mathbb{R}^N$ and susceptibility map $\chi \in \mathbb{R}^N$ is given by $\Phi = \mathbf{F}^{-1} \mathbf{D} \mathbf{F} \chi + \eta$. N is the product of the spatial dimensions (N_x, N_y, N_z) , \mathbf{F} is the 3D Discrete Fourier Transform matrix, $\mathbf{D} = \text{diag}(\mathbf{d})$ where $\mathbf{d}[\mathbf{k}] = \frac{1}{3} - \frac{\mathbf{k}^2}{k^2}$, $\mathbf{k} \neq 0$ is the spectrum of the dipole kernel, $\mathbf{k}^2 = \mathbf{k}_x^2 + \mathbf{k}_y^2 + \mathbf{k}_z^2$ with $\mathbf{k}_x, \mathbf{k}_y, \mathbf{k}_z$ being the \mathbf{k} -space coordinates and η is the measurement noise. The problem of estimating χ from Φ is ill-posed. We propose to exploit the common features present in the patches of the susceptibility map and use it as prior information during recovery. Specifically, the redundancies across the patches of χ are captured using a CNN. The recovery of χ from Φ is then formulated as the following regularized optimization problem:

$$\Theta^*, \chi^* = \arg \min_{\Theta, \chi} \|\Phi - \mathbf{F}^{-1} \mathbf{D} \mathbf{F} \chi\|_2^2 + \mu \sum_{(i,j,k)} \|\mathbf{W}_{ijk}(\mathcal{R}_{ijk}(\chi) - f_{\Theta}(z_{ijk}))\|_2^2 \quad (1)$$

In 1, the first term is the data fidelity term, the second term acts as a regularizer and $\mu > 0$ is a regularization parameter. $\mathcal{R}_{ijk}(\chi) \in \mathbb{R}^p$ extracts a patch of size $p_x \times p_y \times p_z$ from the location indexed by (i, j, k) and vectorizes it. $f_{\Theta}(\cdot)$ is a CNN parameterized by the weights Θ and $z_{ijk} \in \mathbb{R}^p$ is the input to the network. According to [15], a deep neural network with randomly initialized weights and random noise as input can be used to fit any degraded image under an observation model. Accordingly, we also assume z_{ijk} to be uniform random noise with variance 0.1. \mathbf{W}_{ijk} is a diagonal matrix where each entry (corresponding to a voxel location) is inversely related to the number of patches covering that voxel. Multiplication by the diagonal matrix is necessary to ensure that the same μ is applied to every voxel, which will not occur when a stride > 1 is used for patch extraction. We adopt an alternating minimization strategy to solve 1, which decouples it into two simpler sub-problems corresponding to denoising and inversion steps. We iterate between the two steps until convergence is reached. $f_{\Theta}(\cdot)$ is chosen to be a 3D UNet architecture with four encoder and decoder levels with skip connections. In the denoising step, the network weights are initialized using the weights from the previous iteration. They are updated using an ADAM optimizer with a learning rate of 1e-6. We choose a patch size = $64 \times 64 \times 64$ and stride = $32 \times 32 \times 32$. The algorithm was run on a CentOS 7 Linux machine equipped with NVIDIA RTX A6000 GPU.

We validated the proposed method on a dataset corresponding to a healthy subject, which was provided as part of the 2016 QSM reconstruction challenge [14]. The dataset ($160 \times 160 \times 160$) was acquired on a 3T Siemens scanner with an isotropic resolution of 1.06 mm using a 3D Gradient echo sequence. QSM map computed from data acquired from multiple orientations (COSMOS) [16] was used as ground truth. For comparison purposes, QSM maps were recovered using thresholded k-space division (TKD) [17] and regularized approaches using total variation (TV) and total generalized variation (TGV) penalties. The recovered maps corresponded to the lowest root mean square (rmse) with the ground truth.

3 Results

The susceptibility maps corresponding to the different methods are shown in Fig. 11. Clearly, the proposed QSM reconstructions have better delineation of the finer structures such as the inferior sagittal sinus, cortical veins, and the deep veins, which are marked by purple, brown and blue arrows respectively. In addition, the proposed maps retain higher contrast between the gray and white matter structures, especially in the regions enclosed by the green and red boxes (rows 3 and 4 in Fig. 11). Also, the proposed maps are less noisy and more faithful to the ground truth when a smaller patch size is employed (see (b) vs (c)). This is because the weights of the network are being optimized for

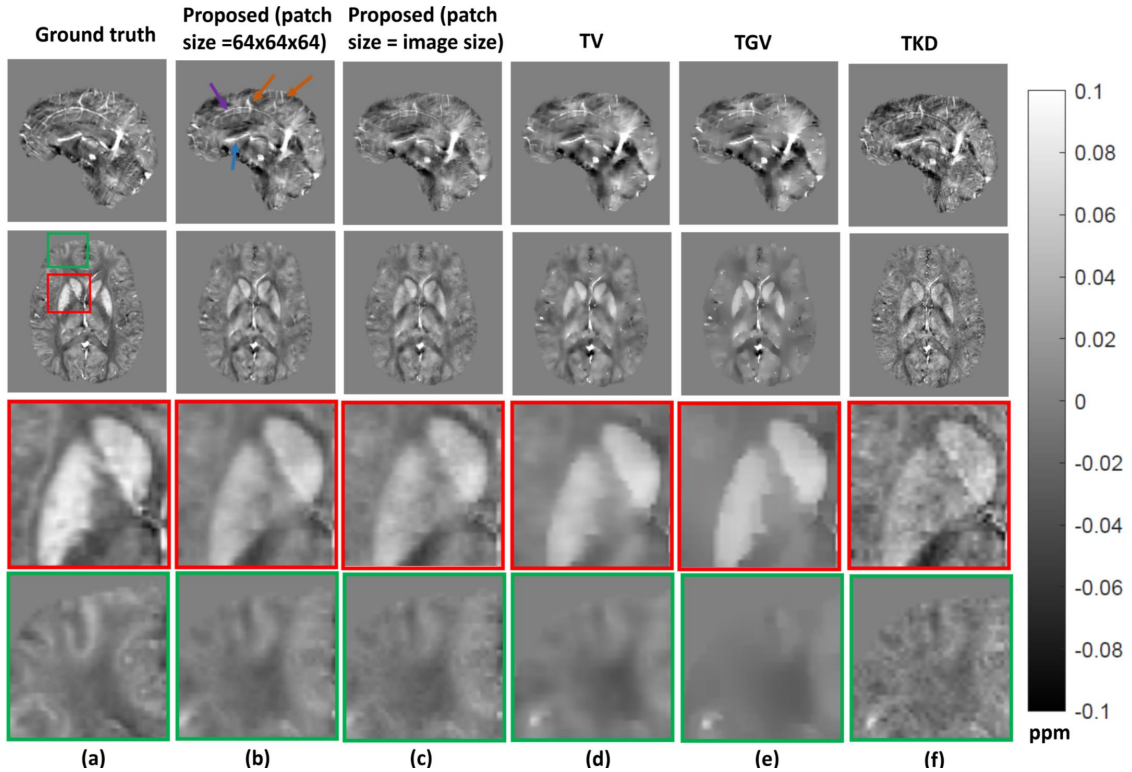


Figure 1: Comparison of the susceptibility maps (sagittal-1st row, axial-2nd row) recovered using different methods: (a) Ground truth, (b) Proposed (patch size = $64 \times 64 \times 64$), (c) Proposed (patch size = image size), (d) Total Variation (TV), (e) Total Generalized Variation (TGV), and (f) Thresholded k-space division (TKD).

multiple smaller patches, which lead to the common features being learned while exhibiting high impedance towards learning noise. However, this comes at the cost of increased computation time. Quantitative metrics, shown in table 11, also indicate that the proposed method provides improved QSM reconstructions compared to the different methods.

Table 1: Comparison of various metrics for different methods

Name	RMSE	SSIM	PSNR
TKD	70.57	0.79	40.55
TGV	61.4	0.83	41.76
TV	62.35	0.84	41.63
Proposed (patch size = image size)	59	0.85	42.1
Proposed (patch size = $64 \times 64 \times 64$)	57.5	0.86	42.32

4 Conclusion

By proposing a subject-specific, unsupervised deep learning formulation for estimating the quantitative susceptibility map, we by-passed the generalization issue pertaining to current deep learning methods. We exploited the common features present in the patches of the map using a deep convolutional network and enforced it as a prior for the QSM inversion problem. We estimated the map by solving a regularized optimization problem using an alternating minimization strategy. As the weights of the network are optimized for multiple smaller patches, the network is more favorable to learn the redundancies across the patches, and will show high resistance to learning noise. Consequently, we observed that the proposed QSM reconstructions have better contrast between gray and white matter, delineation of finer venous structures, and is more faithful to the ground truth compared to the

competing methods. Future work would involve extensive testing on a number of real datasets and validation of the performance through the scores of Neuroradiologists.

5 Potential Negative Societal Impact

The authors do not identify any potential negative impact for this work on the society.

References

- [1] E Mark Haacke, Norman YC Cheng, Michael J House, Qiang Liu, Jaladhar Neelavalli, Robert J Ogg, Asadullah Khan, Muhammad Ayaz, Wolff Kirsch, and Andre Obenaus. Imaging iron stores in the brain using magnetic resonance imaging. *Magnetic resonance imaging*, 23(1):1–25, 2005.
- [2] Jongho Lee, Karin Shmueli, Byeong-Teck Kang, Bing Yao, Masaki Fukunaga, Peter Van Gelderen, Sara Palumbo, Francesca Bosetti, Afonso C Silva, and Jeff H Duyn. The contribution of myelin to magnetic susceptibility-weighted contrasts in high-field MRI of the brain. *Neuroimage*, 59(4):3967–3975, 2012.
- [3] E Mark Haacke, Song Lai, Dmitriy A Yablonskiy, and Weili Lin. In vivo validation of the BOLD mechanism: a review of signal changes in gradient echo functional mri in the presence of flow. *International Journal of Imaging Systems and Technology*, 6(2-3):153–163, 1995.
- [4] Tian Liu, Krishna Surapaneni, Min Lou, Liuquan Cheng, Pascal Spincemaille, and Yi Wang. Cerebral microbleeds: burden assessment by using quantitative susceptibility mapping. *Radiology*, 262(1):269, 2012.
- [5] Tian Liu, Cynthia Wisnieff, Min Lou, Weiwei Chen, Pascal Spincemaille, and Yi Wang. Nonlinear formulation of the magnetic field to source relationship for robust quantitative susceptibility mapping. *Magnetic resonance in medicine*, 69(2):467–476, 2013.
- [6] Ashley K Lotfipour, Samuel Wharton, Stefan T Schwarz, V Gontu, Andreas Schäfer, Andrew M Peters, Richard W Bowtell, Dorothee P Auer, Penny A Gowland, and Nin PS Bajaj. High resolution magnetic susceptibility mapping of the substantia nigra in parkinson’s disease. *Journal of Magnetic Resonance Imaging*, 35(1):48–55, 2012.
- [7] Julio Acosta-Cabronero, Guy B Williams, Arturo Cardenas-Blanco, Robert J Arnold, Victoria Lupson, and Peter J Nestor. In vivo quantitative susceptibility mapping (QSM) in alzheimer’s disease. *PloS one*, 8(11):e81093, 2013.
- [8] John F Schenck and Earl A Zimmerman. High-field magnetic resonance imaging of brain iron: birth of a biomarker? *NMR in Biomedicine: An International Journal Devoted to the Development and Application of Magnetic Resonance In Vivo*, 17(7):433–445, 2004.
- [9] Berkin Bilgic, Audrey P Fan, Jonathan R Polimeni, Stephen F Cauley, Marta Bianciardi, Elfar Adalsteinsson, Lawrence L Wald, and Kawin Setsompop. Fast quantitative susceptibility mapping with l1-regularization and automatic parameter selection. *Magnetic resonance in medicine*, 72(5):1444–1459, 2014.
- [10] Christian Langkammer, Kristian Bredies, Benedikt A Poser, Markus Barth, Gernot Reishofer, Audrey Peiwen Fan, Berkin Bilgic, Franz Fazekas, Caterina Mainero, and Stefan Ropele. Fast quantitative susceptibility mapping using 3d EPI and total generalized variation. *Neuroimage*, 111:622–630, 2015.
- [11] Woojin Jung, Steffen Bollmann, and Jongho Lee. Overview of quantitative susceptibility mapping using deep learning: Current status, challenges and opportunities. *NMR in Biomedicine*, 35(4):e4292, 2022.
- [12] Sai prasad Ravishankar and Yoram Bresler. MR image reconstruction from highly undersampled k-space data by dictionary learning. *IEEE transactions on medical imaging*, 30(5):1028–1041, 2010.

- [13] Muhammad Asim, Fahad Shamshad, and Ali Ahmed. Patchdip: exploiting patch redundancy in deep image prior for denoising. *NeurIPS 2019 Workshop Deep Learning and Inverse Problems*.
- [14] Christian Langkammer, Ferdinand Schweser, Karin Shmueli, Christian Kames, Xu Li, Li Guo, Carlos Milovic, Jinsuh Kim, Hongjiang Wei, Kristian Bredies, et al. Quantitative susceptibility mapping: report from the 2016 reconstruction challenge. *Magnetic resonance in medicine*, 79(3):1661–1673, 2018.
- [15] Dmitry Ulyanov, Andrea Vedaldi, and Victor Lempitsky. Deep image prior. In *Proceedings of the IEEE conference on computer vision and pattern recognition*, pages 9446–9454, 2018.
- [16] Tian Liu, Pascal Spincemaille, Ludovic De Rochefort, Bryan Kressler, and Yi Wang. Calculation of susceptibility through multiple orientation sampling (COSMOS): a method for conditioning the inverse problem from measured magnetic field map to susceptibility source image in MRI. *Magnetic Resonance in Medicine: An Official Journal of the International Society for Magnetic Resonance in Medicine*, 61(1):196–204, 2009.
- [17] Karin Shmueli, Jacco A de Zwart, Peter van Gelderen, Tie-Qiang Li, Stephen J Dodd, and Jeff H Duyn. Magnetic susceptibility mapping of brain tissue in vivo using MRI phase data. *Magnetic Resonance in Medicine: An Official Journal of the International Society for Magnetic Resonance in Medicine*, 62(6):1510–1522, 2009.